

Structural and object detection for phosphene images

Melani Sanchez-Garcia¹, Ruben Martinez-Cantin^{1,2,3}, Jose J. Guerrero¹

¹ I3A, Universidad de Zaragoza, Spain

² Centro Universitario de la Defensa, Zaragoza, Spain

³ SigOpt Inc., San Francisco, CA

(mesangar,rmcantin,josechu.guerrero)@unizar.es

Abstract. Prosthetic vision based on phosphenes is a promising way to provide visual perception to some blind people. However, phosphenic images are very limited in terms of spatial resolution (e.g.: 32 x 32 phosphene array) and luminance levels (e.g.: 8 gray levels), which results in the subject receiving very limited information about the scene. This requires using high-level processing to extract more information from the scene and present it to the subject with the phosphenes limitations. In this work, we study the recognition of indoor environments under simulated prosthetic vision. Most research in simulated prosthetic vision is performed based on static images, while very few researchers have addressed the problem of scene recognition through video sequences. We propose a new approach to build a schematic representation of indoor environments for phosphene images. Our schematic representation relies on two parallel CNNs for the extraction of structural informative edges of the room and the relevant object silhouettes based on mask segmentation. We have performed a study with twelve normally sighted subjects to evaluate how they were able to recognize the rooms by presenting phosphenic images and videos with our method. We show how our method is able to increase the recognition ability of the user from $\sim 75\%$ using alternative methods to 90% using our approach.

Keywords: Computer vision, Deep learning, Visual prosthesis, Simulated prosthetic vision

1 Introduction

The use of visual prostheses has become the only way to generate visual stimuli for certain conditions of visual impairment such as in *retinitis pigmentosa* or *age-related macular degeneration*. These prostheses rely on electrical simulation of the visual pathway using implanted microelectrodes. The electrodes stimulate the retinal ganglion cells based on the light patterns detected in the field of vision [1]. The resulting vision is a set of phosphenes displayed in a restricted portion of the visual field. The patients then has to learn how to interpret the incoming visual sensations in order to 'see'. Unfortunately, there are still some restrictions, such as limited visual acuity [2] because of the spatial, temporal

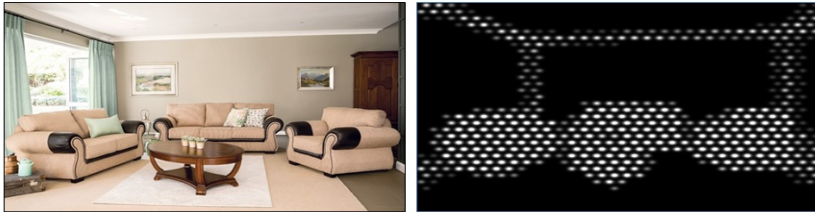


Fig. 1. From input to output. Left: Original image. Right: Simulated prosthetic vision with 1024 phosphenes

and luminance resolution of the electrodes. The main issue is the limitation on the number of implantable electrodes due to medical procedures and biological constraints. Most research has been focused on increasing the information bandwidth by adjusting the implant or performing some previous image processing which is another important factor to improve the quality of prosthetic vision. In this way, the salient features of the image can be detected and emphasized for display maximizing the information content at low-resolution [3,4,5]. Others have focused on optimizing the geometry of the set of electrodes which affects to the density of phosphene organization within the available visual field [2]. Head movements also turns out to be a strategy to improve the visual perception allowing greater ease in the recognition of scenes or objects with a limited field of view [6].

In order to reduce the cost of evaluation and simplify the prototype design and processing blocks, most researchers use Simulated Prosthetic Vision (SPV). SPV offers an alternative way of adjusting implant designs and estimate the minimal information requirements to improve the perceptual quality of the prosthetic wearer. A number of daily tasks such as safely walking [7,5], text reading [8] and object recognition and localization [9,10] have been studied under SPV. Most of these approaches of SPV are focused on computer vision strategies to enhance the perceptions preserving the relevant content of the image [11,12]. These methods are usually based in low level processing of the image, which reduces the amount of information to be transmitted. Furthermore, these techniques have been usually studied and evaluated with static images. Few researchers have addressed the issue of the recognition through video sequences [13], which is an important aspect of real vision.

High level image processing, such as object and place recognition, is becoming feasible even in general settings and with temporal constraints like those presented in prosthetic vision. For such tasks, deep learning has revolutionized the field of computer vision from the seminal work of LeCun et al. [14] to the groundbreaking results of Krizhevsky et al. [15], becoming a key area of research. A diverse range of deep learning algorithms are being employed in the field of computer vision. Concretely, convolutional neural networks (CNNs) have achieved state of the art results in different tasks such as object detection [16,17], place recognition [18], layout estimation [19], semantic segmentation [20] and depth

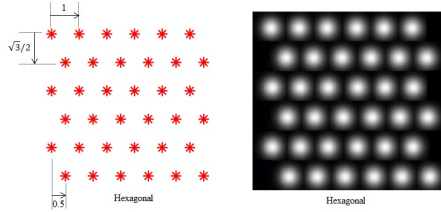


Fig. 2. Simulation of phosphene map. Left: Phosphene configuration to create a regular hexagonal array. Right: Gaussian smoothing applied to the hexagonal array

perception [21]. Deep neural networks can be used to carry out iconic representations of the environment, allowing more useful information in the phosphene image generated.

The contribution of this work is twofold. First, we present a new approach of phosphenic image and video generation based on the combination of relevant object detection and segmentation and the detection of structural edges in indoor scenes. We increase the effectiveness of the phosphenic images by enhancing relevant features in a scene. Both the object segmentation and the structural edges are extracted using CNNs, allowing real time processing for video. Second, we evaluate our iconic representations for scene recognition both with static images and video using SPV. Section 2 describes the process of phosphene generation for simulated prosthesis. Section 3 presents our image processing algorithm. The effectiveness of the proposed representation of scenes is illustrated in Section 4.

2 Simulated prosthetic vision

First, we investigate some requirements necessary for visual prosthesis, such as phosphene pattern, phosphene dropout, field of view, camera/head movement and frame rate.

2.1 Phosphene pattern

We use an hexagonal phosphene map, which is one of the most commonly adopted by SPV in the literature [22]. To carry out the representation of the phosphene map we made several design choices according to the considerations of the real retinal electrodes [23]. The phosphenes of the hexagonal sampling grid are arranged in a 32 x 32 grid (1024 phosphenes), which has been previously considered the lower bound for recognition tasks [24]. The geometry of the array is parameterized as shown in Fig. 2.

Similarly to many SPV studies [22], phosphenes are approximated as grayscale circular dots with a Gaussian luminance profile, as can be seen in Fig. 2. Each phosphene had maximum intensity at the center and tailed off smoothly towards



Fig. 3. Two steps for the representation of our phosphenic approach. The left image shows the original image of an indoor environment. The middle image shows the indoor image represented by an hexagonal phosphene array (phosphenic image). The right image shows the phosphenic image with 10% of dropout

the periphery, following an unnormalized Gaussian function $G(x, y)$ defined as:

$$G(x, y) \propto \exp \left\{ \frac{(x - \mu_x)^2 + (y - \mu_y)^2}{2\sigma^2} \right\} \quad (1)$$

The Gaussian profile is applied to every phosphene resulting in the final image:

$$I(x, y) = A(\mu_x, \mu_y) \cdot G(x, y) \quad (2)$$

where $I(x, y)$ represents the pixel value (grayscale) at the coordinates (x, y) of the stimulus image. $A(\mu_x, \mu_y)$ is the original image after reducing the spatial and luminance resolution to the 32×32 pixels and 8 luminance levels. We assume that the 32×32 pixels are at coordinates (μ_x, μ_y) . The limited gray levels are selected according to number of luminance levels attainable in human trials using retinal prostheses [13,22].

2.2 Phosphene dropout

Human trials in epiretinal prostheses have demonstrated that there was a degree of incomplete phosphene visual field maps (dropout) due to the high threshold required values to elicit phosphenes that were placed in areas with a high proportion of dead nerve cells [25]. This results in a lower resolution than the number of electrode elements. To simulate dropout, we turn off a random 10% of phosphenes on the 32×32 array of the images. The resulting effect can be seen in Fig. 3.

2.3 Field of view and head motion

The size of the field of view (FOV) has a significant influence in performance for mobility, orientation and scene recognition tasks [26]. Large fields of view, such as the visual field in normal vision of humans, allow the exploration of a significant part of the whole visual scene that helps to understand more effectively the visualized scene. However, in prosthetic vision where the resolution is limited to a few phosphenes, a large field of view would imply a deterioration of effective resolution that would affect the recognition of the information [27].

Visual prosthesis currently implanted as the Argus II cover a maximum field of view of 20° [28]. This small field of view makes difficult to carry out tasks such as recognition of whole scenes.

One way to deal with it is to make head movements thus expanding the field of view. Humayun [29] observed that a proper scanning technique can improve upon SPV face recognition, object discrimination and reading. Circular scanning is one of the most head movements that people with visual disability usually perform. It has been demonstrated that scanning in a circular motion more effectively revealed new visual information as compared to separate horizontal and vertical scans [30]. Thus, we capture the video sequence in a circular motion, so that both the central and the peripheral part of the scene were visualized. The purpose of this is to present the subjects more information about the scene, housing a larger field of view through the sequence of frames.

2.4 Frame rate

Some researchers have carried out studies of different tasks with video sequences under simulated prosthetic vision [31,32,33]. For recognition tasks with SPV, the optimal frame rate appears to be around 20 Hz [32]. Experiments with frame rate below 20 Hz seemed insufficient to effectively integrate the sequence of images as a video. In the same way, subjects seemed to mix the images into an almost static image with higher frame rates, lowering the performance in recognition tasks. Thus, we decide to set our videos at 20 Hz. The duration of the videos is approximately 10 seconds in our experiments, doing a closed circular head motion.

3 High level processing for iconic representation

In order to address the schematic representation of indoor environments we need to classify which image regions are interesting in the scene. In this work, we use two different pixel classifiers. First, we use a CNN to find image regions belonging to interesting objects in the scene. That is, we display the *masks of relevant object instances* in order to extract semantic information from the scene [35]. Second, we use a secondary FCN for pixel-wise classification of the *structural informative edges* from the layout of a room. These edges are the edges formed by the intersections of two room faces: two walls, wall and ceiling, etc. Using the resulting labels and masks, we propose two strategies for phosphene generation to enhance the limited visual perception under SPV: a) *Object Masks* (OM), and b) *Structural Informative Edges combined with Object Masks* (SIE-OM) (see Fig. 4).

3.1 Object masks

Silhouettes of certain objects can provide a large amount of information in binary images. Silhouettes can be extracted from object segmentation. For this

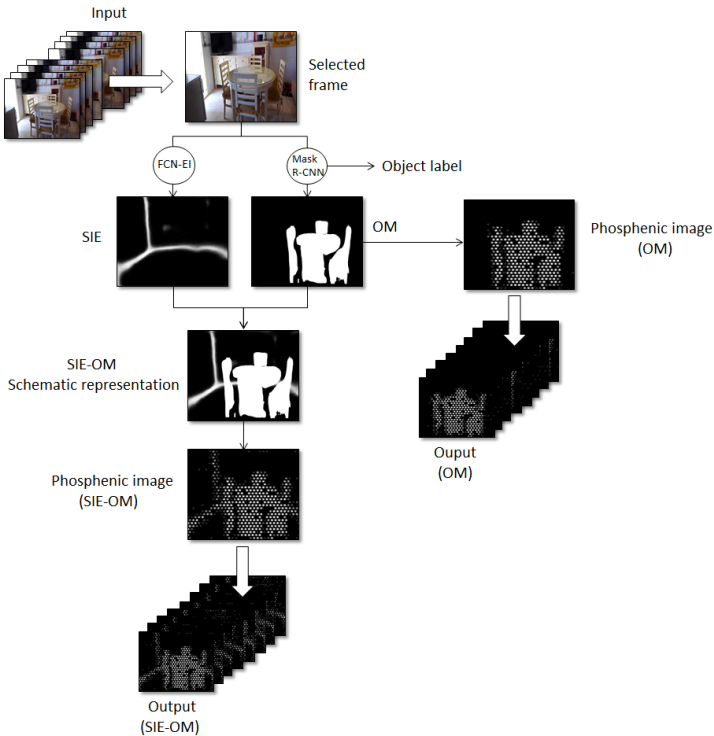


Fig. 4. From an input of frames sequence we use two neural networks algorithms to enhance relevant features in a selected frame. Structural Informative Edges (SIE) are generated from [34] and Objects Masks Segmentation (OM) are generated from [35]. The extracted information is superimposed (SIE-OM) in low resolution to subsequently bring it to a phosphenes pattern to simulate prosthetic vision. Finally, we generate videos with sequences of processed frames

component of our model, we used the object mask extraction from He et al. [35], which is called Mask R-CNN.

This method is composed by a convolutional neural network (CNN), an extension of Faster R-CNN [36]) used for object detection. The structure of Mask R-CNN is a cascade of networks. Following the original Faster R-CNN steps, the first network, called a Region Proposal Network, proposes candidate object bounding boxes. The second, extracts features from each Region of Interest (RoI) using a variant RoI pool, called RoIAlign, from each candidate box and performs classification and bounding-box regression. The result of this step is a double outputs for each candidate object, a class label and a bounding-box offset. The novelty of Mask-RCNN is a third network, a Fully Convolution Network (FCN), that is applied to each region of interest to perform pixel-wise classification to extract the segmentation masks of each object instance. This third network uses various blocks of convolution and max pool layers to first decompress an image of

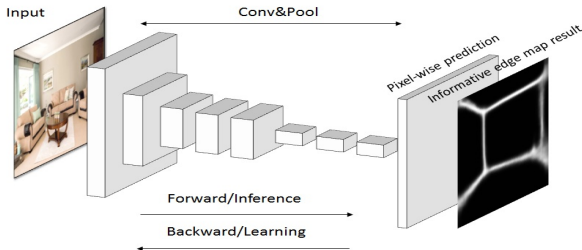


Fig. 5. Fully convolutional network architecture for informative edge map prediction. Note that the object mask prediction given a region of interest have a similar structure.

its original size and it then makes a class prediction. Finally, it uses up sampling and deconvolution layers to resize the image to its original dimensions.

Regarding the loss function for the model, it is composed by the total loss in doing classification, generating bounding box and generating the mask. This approach has been shown to outperform previous state-of-the-art models [37,38]. For this work, we have used a pretrained model on the COCO dataset [35], but we have removed some of the object classes that produced uninformative silhouettes for our purpose.

3.2 Structural edges

Structural edges of rooms are a very interesting source of information to understand the layout of a room in a iconic way, because they provide a sense of perspective and scale and they are easy to track during movement.

Previous works are focused on finding the spatial layout of indoor scenes inferring a 3D box that best fits the room [39], using complex mid and low-level image features or powerful inference procedures. However, the detection of the most informative edges of a room, even those are not always visible remains a challenge. We choose the solution proposed by Fernandez-Labrador et al. [40] that is based on the framework of Mallya et al. [34], which has achieved state-of-the-art results on indoor scene layout prediction by using just edge-based features. This approach directly predict informative edge maps for room layout estimation. Similarly to the pixel classifier for the object masks described in Section 3.1, this method is also based on a FCN for pixel classification (see Fig. 5). Given an image, the FCN determines the informative edge map of an image. This network has the particularity that it is trained for two joint tasks: prediction of the informative edges and geometric context labels. The geometric context labels correspond to different room faces plus an object or cluster label. In this FCN, the total loss is considered as the sum of the two cross-entropy classification losses: for the informative edge label prediction and for the geometric context label prediction.

In a similar way to the previous method, we have used the networks trained with the NYUDv2 RGBD dataset for the 40-class indoor semantic segmentation task of Gupta et al. [41].

The authors also present a couple of inference method which is able to determine the optimal layout. Similarly to the object classes, we chose to ignore that information for the phosphene images, although it could be integrated in future works.

3.3 Phosphene image and video generation

Once the mask of the selected objects and informative edges have been extracted as relevant in the scene, the rest of the information present in the scene was removed. We use the objects masks extracted from the original images to create a schematic representation of the indoor scene (OM). Then, we reduce the resolution of images to 32 x 32. For the (SIE-OM) model, we combine the pixel classification of the object masks with the structural informative edges from Section 3.2.

Finally, we employ a temporal median filter on the video sequence. The use of a temporal median filter ensure temporal consistency and to prevent the flickering effect in the videos. We apply the algorithm across five frames. Starting from the fifth frame, it outputs each pixel by calculating the median of the current frame and the four frames before. Thus, it take five frames and it is determined each pixels probable value, reviewing which pixel is closest matching to its temporal neighbor.

4 Experimental setup

In this section we cover the evaluation of the proposed method for indoor image representation by measuring the ability of recognizing several room types for a set of subjects using the simulated prosthetic vision.

4.1 Ethics statement

All of the experimental process were conducted according to the ethical recommendations of the Declaration of Helsinki. All subjects were informed about the purpose of the experiment. They could discontinue the study at any time.

4.2 Procedure

Subjects had to perform indoor scenes classification task through the visualization of static images and video sequences. For the formal experiment, subjects were seated in front of a monitor (SyncMaster S22B300B Widescreen LED) at a distance of 1 m. We gave verbally a brief introduction of different tasks procedures to all the subjects before the experiment. First, the subjects saw a single image and a video as an example to help them understand the experiment and

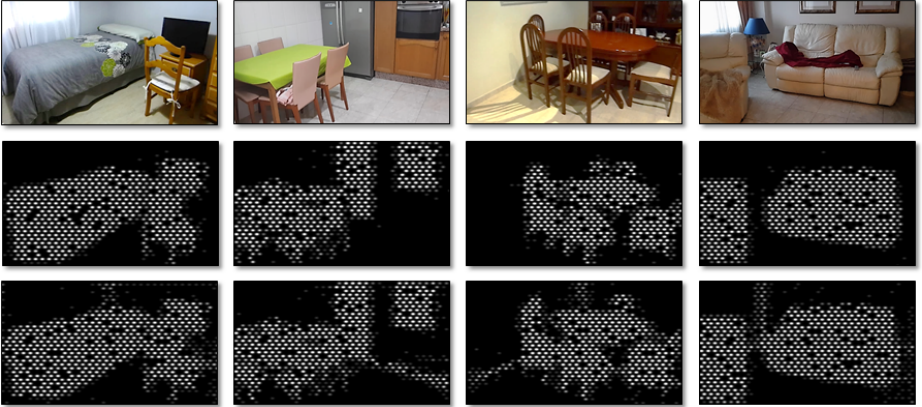


Fig. 6. Each column shows examples of indoor scenes. The first row shows the original image. The middle row shows each type of indoor room processed by OM method. The third row shows shows each type of indoor room processed by SIE-OM method

informing them what would appear in the formal experiment. These examples were not included in the formal experiment. Besides, subjects were informed about the different types of rooms and objects that they were going to see. But they were not informed about the number of objects in each image or video.

The task assigned to the subjects was to recognize an indoor environment among four types of room and the types of object present in each scene. Our selection of indoor scenes included bedrooms, kitchens, living rooms and dining rooms, and the selection of objects is composed by sinks, refrigerators, ovens/microwaves, tables, chairs, TV's/laptops, beds and couches.

All participants had five minutes to become familiar with the experiment procedure and with the examples of processed images and videos. All subjects tested the images prior to the videos. We used image resolution of 32×32 in all the examples. The videos were set to be reproduced at 20 fps, with a duration of 10 s approximately. The visualized scene covered a 20° field of view, based on the available visual field of retinal prosthesis [42].

There were two different tasks in the formal tests. The first task was composed by eight static images and four videos of different indoor environments, each one processed with both methods presented in this document (OM and SIE-OM). We selected two types of images: the first one taken from a central view angle where the most relevant part of the scene is displayed (*Cent*), and another one by randomly selection of a frame of each video (*Rand*). The presentation sequence was randomized for each subject undertaking the study. For this, they had to mark with a cross the boxes of the objects identified in each example. The second task was to identify the type of room to which each example corresponds, i.e. they had to determine room types based on what they were seeing on each phosphenic example. For this, they had to mark with a cross the type of room recognized and the certainty with which they were able to rec-

ognized it according to the Likert ranking. After each test, the next example was configured consecutively. The time allotted for each example was limited to 30 seconds. The whole experiment had an average duration of 6 minutes per subject.

Twelve subjects (two women and ten men) were volunteered in this experiment. The subjects were between 20 and 60 years old. We asked them about their knowledge of computer vision tasks and their possible vision acuities.

5 Results

We compare the two methods present in Section 3, OM and SIE-OM, in two different ways: using *static images* and using *videos*. As commented before, all the scenes were indoor environments.

The results fall into two main sections: object identification and room type recognized tasks. To obtain the results we collect the percentage of *correct* (C) and *incorrect* (I) responses in both tasks. We also analyze the responses of the Likert ranking selected based on the assurance with which they had made the tasks. We assume the responses marked as *definitely yes* (DY), *probably yes* (PY), *maybe* (M) and *probably no* (PN) as the subject had thought that they had recognized the type of room related to the visualized image and video. We also assume that the responses selected as *definitely no* (DN) means that subjects do not understand the type of room witnessed.

First, we gather the responses obtained from each method (OM and SIE-OM) by all the participants, with central and random images (Table 1). The overall results of the tasks for static images and videos are summarized in Table 2. Finally, we test the SIE-OM method with videos separating subjects with different age range: a younger group of ages between 20 and 30 years old and a senior group in the range of 50 to 60 years old. This is shown in Table 4. For the overall results we have include 95% confidence intervals.

We have included two videos as supplementary material, to show the algorithms of the proposed methods running in two indoor rooms: a living room and a kitchen. The videos show both methods (OM and SIE-OM) with all the parameters defined in Section 2.

5.1 Object identification

The random images had the less percentage of objects identified correctly compared with central images, in both OM and SIE-OM methods. Besides, the random images had the high percentage of DN responses, which suggest that some of the images were not understood by the subjects. The main reason may be that these images are not centered in a field of view where all the objects are visualized, which makes their identification difficult. This confirms that static images complicate understanding when all the information of the scene is not present in the field of view. There was no significant difference between OM and SIE-OM methods in the identification score of objects with static images (Table

Table 1. Comparison of responses of static images using OM and SIE-OM methods on object identification and room type recognition tasks. We compared central (Cent) images with random (Rand) images. The assurance of the two methods were evaluated with the Likert ranking

| Method | Object present | | Object missing | | % Correct object identification | % Room type recognized | % Level of Confidence | | | | |
|-------------|----------------|-----|----------------|-----|---------------------------------|------------------------|-----------------------|----|----|----|----|
| | % C | % I | % C | % I | | | DY | PY | M | PN | DN |
| OM Cent | 14 | 6 | 66 | 14 | 80 | 54 | 17 | 33 | 25 | 17 | 8 |
| OM Rand | 7 | 11 | 61 | 21 | 68 | 38 | 0 | 17 | 33 | 17 | 33 |
| SIE-OM Cent | 15 | 7 | 62 | 16 | 77 | 54 | 17 | 42 | 12 | 12 | 17 |
| SIE-OM Rand | 9 | 5 | 67 | 19 | 76 | 54 | 0 | 8 | 42 | 29 | 21 |

Table 2. Responses of static images (Ima) and videos (Vid) using OM and SIE-OM methods on object identification and room type recognition tasks. This meant an increase in the performance of videos task compared to images task, from 54% to 79%, for the task of room recognition using SIE-OM method

| Method | Object present | | Object missing | | % Correct object identification | % Room type recognized | % Level of Confidence | | | | |
|------------|----------------|-----|----------------|-----|---------------------------------|------------------------|-----------------------|----|----|----|----|
| | % C | % I | % C | % I | | | DY | PY | M | PN | DN |
| OM Ima | 11 | 8 | 63 | 18 | 74 ± 5.06 | 46 ± 14.81 | 8 | 25 | 29 | 17 | 21 |
| OM Vid | 14 | 6 | 67 | 13 | 81 ± 7.13 | 67 ± 19.32 | 33 | 33 | 13 | 4 | 17 |
| SIE-OM Ima | 12 | 6 | 65 | 17 | 77 ± 4.80 | 54 ± 13.14 | 8 | 25 | 27 | 21 | 19 |
| SIE-OM Vid | 23 | 2 | 67 | 8 | 90 ± 4.63 | 79 ± 12.78 | 13 | 67 | 16 | 4 | 0 |

2). This suggests that the structural edges do not provide much information in the identification of objects in static images. Moreover, the presence of structural edges in some areas of the images caused subjects to confuse it with objects.

Looking at the results obtained only for videos (Table 2), the total percentage of correct object identification task with SIE-OM method was very high, of 90%, which meant a clear increase compared to static images. Even with the reduced number of subjects in the evaluation, the difference was statistically significant compared to any other method. Moreover, the highest percentage of confidence with which they had performed the task is distributed among the responses of DY and PY, which means that subjects could identify the objects easily.

5.2 Room type classification

We found a significant difference in the classification score of room type between central and random images. The increase in the percentage of success in the room recognition with SIE-OM versus OM method for random images was due to the contours which are necessary to show which part of the scene they are visualizing.

This study provides additional support for the SIE-OM method since this method also had the best percentage of correct responses for the recognition of room type (54%) than the OM method (46%) for static images (Table 2). The data gathered in this task suggest that given information of structural edges, scenes provide useful information when it comes to recognizing the type of room.

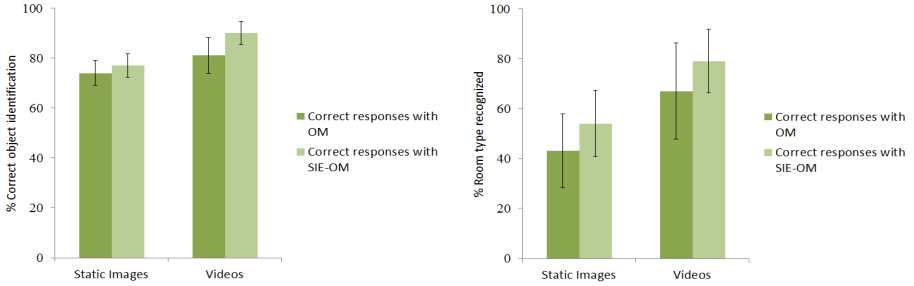


Fig. 7. Correct results of object identification and room type classification tasks were obtained by static images and videos, with responses of OM and SIE-OM methods. The SIE-OM outperforms slightly the OM methods in both cases. The task with videos provided better results than the task of static images. We obtained a 54% with static images and 79% with videos in the task of room type recognition using SIE-OM method

Table 3. Confusion matrix results of room type classification obtained with videos using SIE-OM method. The results show that some subjects confused room types due to the similarity of the objects present in them. Even so, high precision was obtained for our proposed method

| Actual \ Predicted | Bedroom | Kitchen | Dining room | Living room | Recall |
|--------------------|---------|---------|-------------|-------------|--------|
| Bedroom | 0.63 | 0.00 | 0.00 | 0.38 | 62.50 |
| Kitchen | 0.00 | 0.86 | 0.00 | 0.14 | 85.71 |
| Dining room | 0.00 | 0.00 | 0.71 | 0.29 | 71.43 |
| Living room | 0.00 | 0.14 | 0.00 | 0.86 | 85.71 |
| Precision | 100.00 | 85.71 | 100.00 | 51.61 | |

The experiments with videos showed an increase in the percentage of correct responses for both methods. Concretely, it was obtained (79%) versus static images (54%) for SIE-OM method. Furthermore, responses selected as DY and PY with videos comprised higher values compared to the same responses in static images. These differences can be explained in part because the videos aid to have a greater understanding of perception and location of objects and edges of the entire scene.

Table 3 shows the confusion matrix of our model (SIE-OM with videos) in the room type classification. According to the results obtained for the type of room, some subjects confused dining room with living room. This was due to in most of the houses the dining room and the living room are connected as one, so subjects did not know how to differentiate between these rooms. On the other hand, bedroom was confused with living room because of the similarity of shape between some beds and couches. Even so, the recall and precision of our model with videos were high, reaching in some cases 100%.

Furthermore, we analyzed the results of the experiment in two different people age range (Table 4). The results of this part of the test confirmed that the age range does not affect the performance of our method. Subjects were able to

Table 4. Summary of responses of two age ranges of subjects, 20-30 years old and 50-60 years old, with static images and videos using SIE-OM method. The video results outperform static image results in both younger group and senior group. The results are similar in both cases which means that the proposed method does not affect the age range

| Method | Object present | | Object missing | | % Correct object identification | % Room type recognized | % Level of Confidence | | | | |
|--------------|----------------|-----|----------------|-----|---------------------------------|------------------------|-----------------------|----|----|----|----|
| | % C | % I | % C | % I | | | DY | PY | M | PN | DN |
| 20-30 yo Im | 11 | 5 | 72 | 12 | 83 | 50 | 25 | 13 | 37 | 25 | 0 |
| 50-60 yo Im | 8 | 9 | 69 | 14 | 77 | 50 | 0 | 37 | 25 | 13 | 25 |
| 20-30 yo Vid | 22 | 0 | 69 | 9 | 91 | 75 | 25 | 75 | 0 | 0 | 0 |
| 50-60 yo Vid | 22 | 0 | 69 | 9 | 91 | 75 | 0 | 25 | 50 | 25 | 0 |

recognize the same percentage of room type with images and videos, and there was only a small difference in the object identification. Talking about the level of confidence, the senior group had less confidence to understanding the information with static images than the younger group, marking 25% of the answers as DN, although the results obtained are practically the same for both age ranges of subjects.

6 Conclusions

Visual prosthesis research has made significant progress on improving visual perception for blind people. However, there are still some technical limitations, such as spatial and luminance resolution, that needs to be addressed. In this work, we have focused on adding a high-level processing layer to the external images captured by the device in order to increase the information that it is transferred to the subject through the prosthesis. For that purpose, we have used two pixel-wise classifiers for relevant information: structural edges in indoor scenes and relevant object masks. Furthermore, we have evaluated our method, both with static images and video sequences using simulated prosthetic vision.

Using video scenes, even with small movements, subjects were able to obtain a higher percentage of success compared with the static images. Furthermore, subjects were able to recognize the scene displayed with more confidence with the head movement through the video. Besides, it has been demonstrated that structural edges provide useful information when it comes to recognizing the room type. This meant in a higher performance in the SIE-OM method compared to the OM method. In summary, the subject could understand and recognize different indoor environments under the considerations of prosthetic vision.

ACKNOWLEDGEMENTS

This work was supported by project DPI2015-65962-R (MINECO/FEDER, UE) and BES-2016-078426 (MINECO).

References

1. Luján Villarreal, D.: Toward pixel-wise vision in epiretinal visual prosthesis. PhD thesis, Technische Universität Hamburg-Harburg (2017)
2. Chen, S., Lovell, N., Suaning, G.: Effect on prosthetic vision visual acuity by filtering schemes, filter cut-off frequency and phosphene matrix: a virtual reality simulation. In: Engineering in Medicine and Biology Society, 2004. IEMBS'04. 26th Annual International Conference of the IEEE. Volume 2., IEEE (2004) 4201–4204
3. Wang, J., Wu, X., Lu, Y., Wu, H., Kan, H., Chai, X.: Face recognition in simulated prosthetic vision: face detection-based image processing strategies. *Journal of neural engineering* **11**(4) (2014) 046009
4. McCarthy, C., Walker, J.G., Lieby, P., Scott, A., Barnes, N.: Mobility and low contrast trip hazard avoidance using augmented depth. *Journal of neural engineering* **12**(1) (2014) 016003
5. Perez-Yus, A., Bermudez-Cameo, J., Lopez-Nicolas, G., Guerrero, J.J.: Depth and motion cues with phosphene patterns for prosthetic vision. In: Proceedings of the IEEE International Conference on Computer Vision. (2017) 1516–1525
6. Chen, S., Hallum, L., Suaning, G., Lovell, N.: A quantitative analysis of head movement behaviour during visual acuity assessment under prosthetic vision simulation. *Journal of neural engineering* **4**(1) (2007) S108
7. Vergnieux, V., Macé, M.J.M., Jouffrais, C.: Wayfinding with simulated prosthetic vision: Performance comparison with regular and structure-enhanced renderings. In: Engineering in Medicine and Biology Society (EMBC), 2014 36th Annual International Conference of the IEEE, IEEE (2014) 2585–2588
8. Vurro, M., Crowell, A.M., Pezaris, J.S.: Simulation of thalamic prosthetic vision: reading accuracy, speed, and acuity in sighted humans. *Frontiers in human neuroscience* **8** (2014) 816
9. Hu, J., Xia, P., Gu, C., Qi, J., Li, S., Peng, Y.: Recognition of similar objects using simulated prosthetic vision. *Artificial organs* **38**(2) (2014) 159–167
10. Macé, M.J.M., Guivarch, V., Denis, G., Jouffrais, C.: Simulated prosthetic vision: The benefits of computer-based object recognition and localization. *Artificial organs* **39**(7) (2015)
11. Barriga-Rivera, A., Suaning, G.J.: Digital image processing for visual prosthesis: Filtering implications. In: Engineering in Medicine and Biology Society, EMBC, 2011 Annual International Conference of the IEEE, IEEE (2011) 4860–4863
12. Ayton, L.N., Luu, C.D., Bentley, S.A., Allen, P.J., Guymer, R.H.: Image processing for visual prostheses: a clinical perspective. In: Image Processing (ICIP), 2013 20th IEEE International Conference on, IEEE (2013) 1540–1544
13. Wang, J., Lu, Y., Gu, L., Zhou, C., Chai, X.: Moving object recognition under simulated prosthetic vision using background-subtraction-based image processing strategies. *Information Sciences* **277** (2014) 512–524
14. LeCun, Y., Boser, B., Denker, J.S., Henderson, D., Howard, R.E., Hubbard, W., Jackel, L.D.: Backpropagation applied to handwritten zip code recognition. *Neural computation* **1**(4) (1989) 541–551
15. Krizhevsky, A., Sutskever, I., Hinton, G.E.: Imagenet classification with deep convolutional neural networks. In: Advances in Neural Information Processing Systems (NIPS). (2012)
16. Anisimov, D., Khanova, T.: Towards lightweight convolutional neural networks for object detection. In: Advanced Video and Signal Based Surveillance (AVSS), 2017 14th IEEE International Conference on, IEEE (2017) 1–8

17. Eitel, A., Springenberg, J.T., Spinello, L., Riedmiller, M., Burgard, W.: Multi-modal deep learning for robust rgb-d object recognition. In: Intelligent Robots and Systems (IROS), 2015 IEEE/RSJ International Conference on, IEEE (2015) 681–687
18. Chen, Z., Jacobson, A., Sünderhauf, N., Upcroft, B., Liu, L., Shen, C., Reid, I., Milford, M.: Deep learning features at scale for visual place recognition. In: Robotics and Automation (ICRA), 2017 IEEE International Conference on, IEEE (2017) 3223–3230
19. Dasgupta, S., Fang, K., Chen, K., Savarese, S.: Delay: Robust spatial layout estimation for cluttered indoor scenes. In: Proceedings of the IEEE Conference on Computer Vision and Pattern Recognition. (2016) 616–624
20. Gu, J., Wang, Z., Kuen, J., Ma, L., Shahroudy, A., Shuai, B., Liu, T., Wang, X., Wang, G., Cai, J., et al.: Recent advances in convolutional neural networks. Pattern Recognition (2017)
21. Fácil, J.M., Concha, A., Montesano, L., Civera, J.: Single-view and multi-view depth fusion. IEEE Robotics and Automation Letters **2**(4) (2017) 1994–2001
22. Chen, S.C., Suaning, G.J., Morley, J.W., Lovell, N.H.: Simulating prosthetic vision: I. visual models of phosphenes. Vision research **49**(12) (2009) 1493–1506
23. Weiland, J.D., Humayun, M.S.: A biomimetic retinal stimulating array. IEEE engineering in medicine and biology magazine **24**(5) (2005) 14–21
24. Zhao, Y., Lu, Y., Tian, Y., Li, L., Ren, Q., Chai, X.: Image processing based recognition of images with a limited number of pixels using simulated prosthetic vision. Information Sciences **180**(16) (2010) 2915–2924
25. Humayun, M.S., Weiland, J.D., Fujii, G.Y., Greenberg, R., Williamson, R., Little, J., Mech, B., Cimarusti, V., Van Boemel, G., Dagnelie, G., et al.: Visual perception in a blind subject with a chronic microelectronic retinal prosthesis. Vision research **43**(24) (2003) 2573–2581
26. Fornos, A.P., Sommerhalder, J., Pittard, A., Safran, A.B., Pelizzone, M.: Simulation of artificial vision: Iv. visual information required to achieve simple pointing and manipulation tasks. Vision research **48**(16) (2008) 1705–1718
27. Arens-Arad, T., Farah, N., Ben-Yaish, S., Zlotnik, A., Zalevsky, Z., Mandel, Y.: Head mounted dmd based projection system for natural and prosthetic visual stimulation in freely moving rats. Scientific reports **6** (2016) 34873
28. Stronks, H.C., Dagnelie, G.: The functional performance of the argus ii retinal prosthesis. Expert review of medical devices **11**(1) (2014) 23–30
29. Humayun, M.S.: Intraocular retinal prosthesis. Transactions of the American Ophthalmological Society **99** (2001) 271
30. Chen, S., Hallum, L., Suaning, G., Lovell, N.: Psychophysics of prosthetic vision: I. visual scanning and visual acuity. In: Engineering in Medicine and Biology Society, 2006. EMBS'06. 28th Annual International Conference of the IEEE, IEEE (2006) 4400–4403
31. Han, T., Li, H., Lyu, Q., Zeng, Y., Chai, X.: Object recognition based on a foreground extraction method under simulated prosthetic vision. In: Bioelectronics and Bioinformatics (ISBB), 2015 International Symposium on, IEEE (2015) 172–175
32. Kim, H.S., Park, K.S.: Spatiotemporal pixelization to increase the recognition score of characters for retinal prostheses. Sensors **17**(10) (2017) 2439
33. Zhao, Y., Geng, X., Li, Q., Jiang, G., Gu, Y., Lv, X.: Recognition of a virtual scene via simulated prosthetic vision. Frontiers in bioengineering and biotechnology **5** (2017) 58

34. Mallya, A., Lazebnik, S.: Learning informative edge maps for indoor scene layout prediction. In: Proceedings of the IEEE International Conference on Computer Vision. (2015) 936–944
35. He, K., Gkioxari, G., Dollár, P., Girshick, R.: Mask R-CNN. In: Computer Vision (ICCV), 2017 IEEE International Conference on, IEEE (2017) 2980–2988
36. Girshick, R.: Fast R-CNN. arXiv preprint arXiv:1504.08083 (2015)
37. Dai, J., He, K., Sun, J.: Instance-aware semantic segmentation via multi-task network cascades. In: Proceedings of the IEEE Conference on Computer Vision and Pattern Recognition. (2016) 3150–3158
38. Li, Y., Qi, H., Dai, J., Ji, X., Wei, Y.: Fully convolutional instance-aware semantic segmentation. arXiv preprint arXiv:1611.07709 (2016)
39. Hedau, V., Hoiem, D., Forsyth, D.: Recovering the spatial layout of cluttered rooms. In: Computer vision, 2009 IEEE 12th international conference on, IEEE (2009) 1849–1856
40. Fernandez-Labrador, C., Facil, J.M., Perez-Yus, A., Demonceaux, C., Guerrero, J.J.: Panoram: From the sphere to the 3d layout. arXiv preprint arXiv:1808.09879 (2018)
41. Gupta, S., Arbelaez, P., Malik, J.: Perceptual organization and recognition of indoor scenes from rgb-d images. In: Computer Vision and Pattern Recognition (CVPR), 2013 IEEE Conference on, IEEE (2013) 564–571
42. Zhou, D.D., Dorn, J.D., Greenberg, R.J.: The argus® ii retinal prosthesis system: An overview. In: Multimedia and Expo Workshops (ICMEW), 2013 IEEE International Conference on, IEEE (2013) 1–6